

UDK 621.315.592

Non-trivial dependence of spectral characteristics of excitons in quantum wells on the resonant optical excitation power

© D.F. Mursalimov¹, A.V. Mikhailov¹, A.S. Kurdyubov¹, A.V. Trifonov^{1,2}, I.V. Ignatiev¹

¹ St. Petersburg State University,
198504 St. Petersburg, Russia

² Technische Universität Dortmund,
4421 Dortmund, Germany

E-mail: d.mursalimov@yahoo.com

Received April 12, 2021

Revised April 19, 2021

Accepted April 19, 2021

Basic exciton parameters, such as the energy of exciton transition and the radiative and nonradiative broadenings, are experimentally studied by means of reflectance spectroscopy for a heterostructure with a 14-nm GaAs/AlGaAs quantum well. Particular attention is paid to the nonradiative broadening which is sensitive to densities of free carriers and long-lived nonradiative excitons. A sublinear increase of the broadening of the heavy-hole and light-hole exciton resonances is observed when the light-hole exciton resonance is excited with increasing power. A simple model is developed, which allows one to well reproduce the observed dependence.

Keywords: exciton, quantum well, nonradiative broadening.

DOI: 10.21883/SC.2022.13.53888.43

1. Introduction

Currently, the technologies of growing GaAs-based heterostructures allow producing samples of exceptionally high quality. Such structures allows one to study fundamental characteristics of the excitons, namely the energy of exciton transitions, the strengths of light-exciton and exciton-phonon interactions, etc. These studies are important both for verification of exciton models in the heterostructures with quantum wells (QW) and for refinement of the parameters of these models. Further development of these studies could allow using the exciton as a sensitive probe for the QW heterostructures [1].

Beside optically active bright excitons, the optical excitation can generate other quasi-particles, such as free electrons and holes, nonradiative excitons, trions, biexcitons and other bound states of the particles. As a result, the excitons observed in the reflectance or photoluminescence (PL) spectra are not free (isolated), as they are influenced by other quasi-particles generated by the optical excitation. Their influence can be limited by reducing the power of the optical excitation. However, even the low power of the non-resonant excitation required to observe exciton PL generates a reservoir of free carriers and long-lived excitons [2]. The latter propagate along the QW layer with a wave vector K exceeding the light wave vector K_c in the QW material. Such excitons do not interact with light (they are called dark or nonradiative excitons) [3–5] and in high-quality heterostructures their lifetime reach dozens of nanoseconds [2]. Meanwhile for bright excitons with $K < K_c$ the characteristic recombination time is measured in dozens of picoseconds [6]. Significant difference in the

lifetimes results in the fact that two-dimensional density of the nonradiative excitons in the reservoir exceeds the density of the radiative excitons by several orders of magnitude. Interaction of bright excitons with the reservoir significantly impacts their spectral characteristics. Particularly, exciton-exciton scattering results in either interruption of recombination of an electron-hole pair, or a dephasing of the radiative state [7], which manifests itself in broadening of the exciton resonances.

In this work we experimentally study properties of excitons in a high-quality GaAs heterostructure by a reflection spectroscopy. The power dependences of the fundamental spectral characteristics of the excitons have been measured at the resonant optical excitation. A simple and clear model has been developed to describe the experimentally observed sublinear dependence of broadening of the exciton resonance on the excitation power.

2. Experiment and processing of results

The studied structure was grown by molecular beam epitaxy (MBE) on a n -type GaAs (001) substrate. The heterostructure includes a 14-nm-wide QW, which was grown between $\text{Al}_x\text{Ga}_{1-x}\text{As}$ barriers with a small aluminum content, $x \approx 3\%$. The high quality of the sample is due to the low content of aluminum minimizing the number of dislocations [1]. The sample was cooled in a closed-cycle cryostat to the temperature $T \approx 5\text{ K}$.

The reflectance spectra were measured at a small incidence angle of the probe beam. The probing was done by using spectrally wide pulses of the titanium-sapphire laser with the duration of about 100 fs. Reflectance

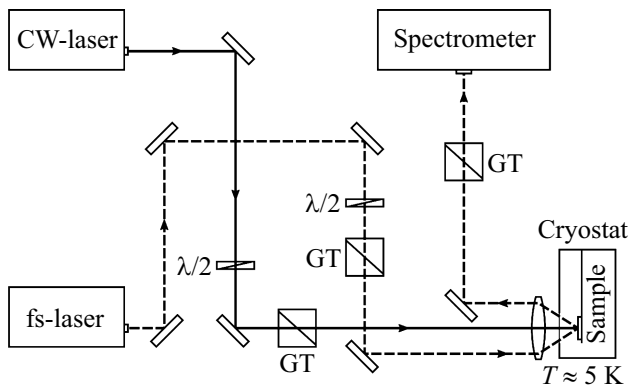


Figure 1. The experimental setup: fs-laser — the pulsed laser, CW-laser — continuous wave laser, GT — the Glan–Taylor prism.

spectra were analyzed by using the spectrometer with the diffraction grating of 1800 lines/mm and a focus distance of 550 mm and detected by a liquid-nitrogen-cooled CCD matrix. The experimental setup is shown in Fig. 1. In our experiments the reservoir of nonradiative excitons was created by using an additional optical excitation (pumping) with a continuous titanium-sapphire laser. It was tuned in resonance with the light exciton optical transition in the studied QW. The pump beam was directed at normal incidence to the sample surface and polarized orthogonally to the probe beam. A Glan–Taylor prism was placed at the spectrometer entrance to prevent scattering of the pumping light on the CCD matrix. A small residual signal from the scattered light of the pump beam was accumulated separately and subtracted at each spectrum measurement. The measurements conducted in such a way are characterized by high reliability and reproducibility. The powers of the laser beams were adjusted by rotating the $\lambda/2$ phase plates placed in front of the Glan–Taylor prisms.

The spectrum of the probe beam reflected from the sample has a wide profile well approximated by the Gaussian function with a half-width at the half-maximum of 10 meV. On top of this background spectrum the narrow resonances were observed, which correspond to a light (Xlh) and heavy (Xhh) exciton. The sample reflectance can be obtained by normalizing the spectrum of the reflected beam by the Gaussian profile of the probe pulse taking into account a surface reflection coefficient. A typical reflection spectrum is shown in Fig. 2.

The exciton lines were shaped as single peaks due to optimal selection of the thickness of the top barrier layer of the QW $L_{\text{top}} \approx 230$ nm. The length of the optical path in the layer $L_{\text{opt}} = L_{\text{top}}n(\text{GaAs}) \approx 830$ nm (n is the refraction index) is close to wavelengths of the exciton resonances. It results in constructive interference of light reflected from the QW layer and the sample surface.

The spectral width of the resonances is extremely sensitive to conditions of the optical excitation. At low power of the probe beam of about $1 \mu\text{W}$ per an area of the laser spot 10^{-4} cm^2 the width of the resonance line Xhh without

pumping is $\Delta E = 185 \mu\text{eV}$, which indicates a high quality of the sample. Additional illumination by the continuous laser results in substantial broadening of the resonances (see Fig. 2).

The shape of the exciton resonance can be modeled within the framework of a non-local dielectric response theory, which is described in the monograph of E.I. Ivchenko [8]. This model was used to analyze the experimental data in many papers (for example [1,2,9–12]). The amplitude reflection coefficient of the QW layer near the exciton resonance frequency ω_X reads as

$$r_{\text{QW}}(\omega) = \frac{i\Gamma_{\text{R}}}{\omega_X - \omega - i(\Gamma_{\text{R}} + \Gamma_{\text{NR}})}, \quad (1)$$

where Γ_{R} and Γ_{NR} are radiative and nonradiative damping rates of excitons, respectively. The intensity of the reflected radiation also depends on the amplitude reflection coefficient of the sample surface r_s and the reflectance is expressed as

$$R(\omega) = \left| \frac{r_s + r_{\text{QW}}(\omega)e^{i2\phi}}{1 + r_s r_{\text{QW}}(\omega)e^{i2\phi}} \right|^2, \quad (2)$$

where ϕ is phase change of the light wave when passing through the barrier to the middle of the QW layer.

The equations (1), (2) were used to fit the spectra shown in Fig. 2. It is clear that the analytical curves exactly describe all features of the resonances. It should be noted that the fitting curves well reproduce the Lorentz shape of the resonances with slowly decaying wings. This indicates only a negligible inhomogeneous broadening exists in the system. Otherwise, the shape wing behavior would be characterized by a faster drop, i.e. the Gaussian shape.

The good agreement of the experimental and theoretical curves allows determination of the main parameters of the

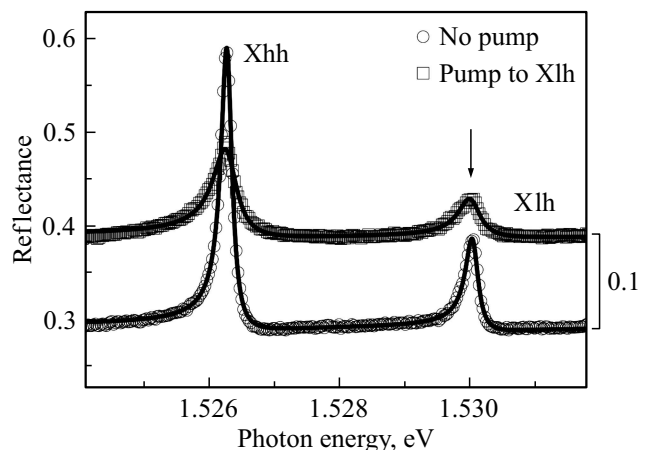


Figure 2. Reflectance spectra of the studied structure measured without pumping (the lower circle-marked curve) and with additional excitation into the light exciton resonance (the upper square-marked curve). The upper spectrum is shifted by 0.1 for visual clarity. The solid lines are approximations according to the formulas (1), (2).

exciton resonances: radiative ($\hbar\Gamma_R$) and nonradiative ($\hbar\Gamma_{NR}$) broadenings, as well as the exciton energy ($\hbar\omega_X$) with accuracy from several to fractions of μeV . It should be noted that the obtained values of the fitting parameters still could have some systematic errors, which, however, do not depend on the conditions of the optical excitation and thereby do not hinder the study of power dependences. The lower spectra in Fig. 2 (without pumping) has the following parameters of the resonance Xhh: $\hbar\Gamma_R = 37\mu\text{eV}$, $\hbar\Gamma_{NR} = 44\mu\text{eV}$ and $\hbar\omega_X = 1.526278\text{ eV}$. Determination of the value of the radiative broadening $\hbar\Gamma_R$ from the experiment requires exact measurement of the surface reflectance, which raises difficulties, as the sample surface is not perfect. That is why the reflectance was selected so that the radiative broadening value might coincide with the results of the microscopic calculation: $\hbar\Gamma_R = 37\mu\text{eV}$ [12,13]. For the resonance Xlh the energy $\hbar\omega_X = 1.530056\text{ eV}$ and the radiative broadening $\hbar\Gamma_R = 15\mu\text{eV}$, which is about 2.5 times smaller than for the Xhh.

The homogeneous nonradiative broadening $\hbar\Gamma_{NR}$ of the exciton resonances is caused by interaction (scattering) of the photo-generated excitons (created by the probe beam) by other quasi-particles of the system: free carriers, phonons, radiative and nonradiative excitons [1,2]. As it is clear from the Fig. 2, such interaction results in substantial increase in $\hbar\Gamma_{NR}$ of the resonance Xhh, which reaches $200\mu\text{eV}$ at relatively small power density $6\text{ W}\cdot\text{cm}^{-2}$ of pumping in the Xlh resonance. The high sensitivity of the nonradiative broadening to such scattering processes allows studying the exciton-exciton interaction in detail.

We have analyzed the parameters of the exciton resonances at continuous pumping into the resonance Xlh. For each pumping power, the reflectance spectra have been measured and processed using the Eqs. (1), (2). Figures 3, 4 show the dependences of the radiative and nonradiative broadenings on the pumping power for the Xhh and Xlh resonances, respectively.

As one can see the parameters are smoothly changing with the increase in the pumping power: the radiative broadening is sub-linearly dropping, while the nonradiative one is sub-linearly increasing. We believe that such behavior is due to the interaction of the bright excitons with the exciton reservoir. The decreased radiative broadening is attributed to depopulation of the vacuum state of excitons due to their accumulation in the reservoir.

The density of the Xlh-excitons generated by the continuous pumping is determined by the power density of the exciting photons and the absorption coefficient α at the excitation frequency. The latter can be expressed as [8]

$$\alpha_{Xlh}(\omega) = \frac{2\Gamma_R\Gamma_{NR}}{(\omega_{Xlh} - \omega)^2 + (\Gamma_R + \Gamma_{NR})^2}. \quad (3)$$

By substituting the power dependences of the broadenings Xlh (Fig. 4) into the formula (3), we can obtain the dependence of the absorption coefficient in the maximum of the resonance Xlh ($\alpha_{Xlh} = \alpha_{Xlh}(\omega_{Xlh})$, see Fig. 5). Evidently,

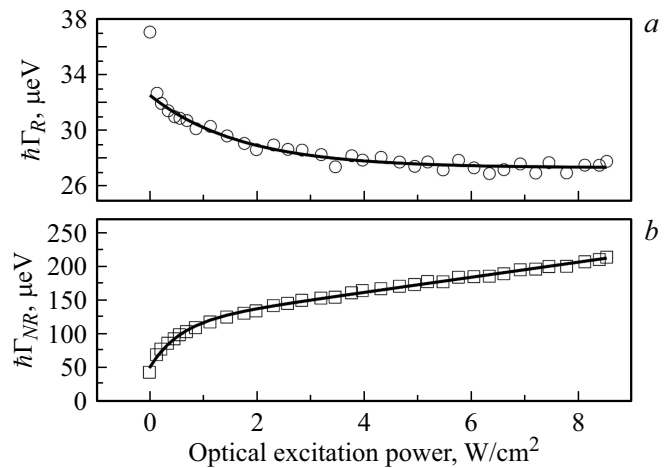


Figure 3. Radiative (a) and nonradiative (b) broadenings of the Xhh resonance at continuous excitation in the Xlh. The solid line is an approximation by the phenomenological dependence $f = A[1 - \exp(P_{exc}/P_0)] + BP_{exc} + C$.

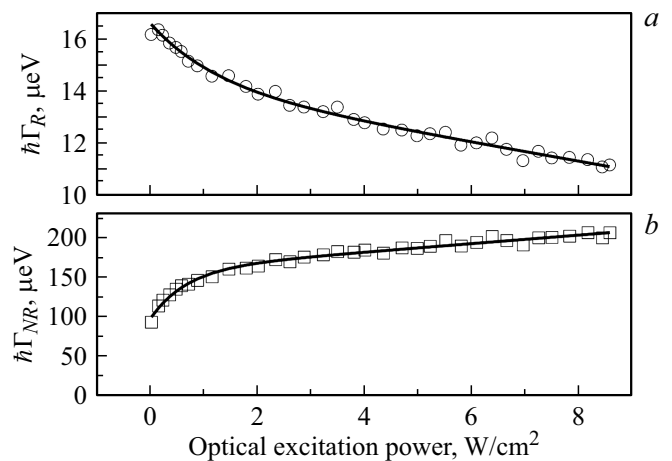


Figure 4. Radiative (a) and nonradiative (b) broadenings of the Xlh resonance at continuous excitation in the Xlh. The solid line is an approximation by the phenomenological dependence $f = A[1 - \exp(P_{exc}/P_0)] + BP_{exc} + C$.

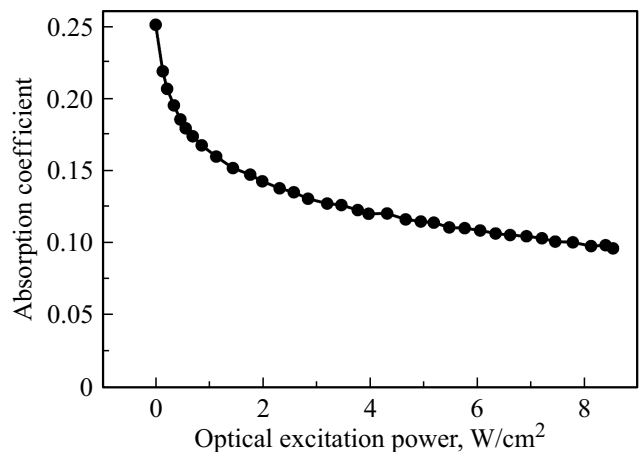


Figure 5. Dependence of the absorption coefficient in the maximum of the resonance Xlh as calculated by the formula (3).

the absorption coefficient significantly decreases with the increase in the pumping power, which is mainly due to significant increase in $\hbar\Gamma_{NR}$.

3. Analysis of the power dependence of the nonradiative broadening

We have analyzed the nonradiative broadening within the framework of a model of dynamic processes, which is developed in [14]. Resonant excitation into the light exciton resonance generates radiative excitons which either quickly relax by emitting a photon (the rate Γ_R), or scatter to the states outside the light cone. In case of the continuous excitation the scattering is predominantly due to interaction with acoustic phonons (with the rate γ_{phon}). A ratio of the rates $f = \gamma_{\text{phon}}/(\Gamma_R + \gamma_{\text{phon}})$ determines the fraction of the nonradiative excitons. Thus, the reservoir filling rate can be written as

$$P_{Xlh} = \alpha_{Xlh} N_{\text{phot}} f. \quad (4)$$

Here, $N_{\text{phot}} = AP_{\text{exc}}/(\hbar\omega_{Xlh})$ is the number of the photons (in $\text{cm}^{-2} \cdot \text{s}^{-1}$), that reached the QW layer, P_{exc} is the power of the optical excitation. The transmission coefficients of the cryostat window and the sample surface — t_w and t_s , respectively, are taken into account in the factor $A = t_w t_s$.

As a result of the scattering light excitons can pass either to the dispersion branch of the heavy excitons (with the rate γ_{Xhh}), or dissociate into electron and hole (with the rate γ_{eh}). The latter play an important role in the model under consideration: after scattering by free carriers nonradiative excitons return into the light cone where they recombine with emission of photons. This bimolecular process results in depopulation of the exciton reservoir and is characterized by the rate κ_c . In turn free electrons and holes can combine into excitons, thereby refilling the reservoir (the bimolecular rate κ_{ex}). As a result, the dynamic equilibrium is established in the system.

The dynamics of the excitons and charge carriers in the reservoir is described by the following system of the equations:

$$\begin{cases} \frac{dn_{Xlh}}{dt} = P_{Xlh} - (\gamma_{Xhh} + \gamma_{eh})n_{Xlh} \\ \frac{dn_e}{dt} = \frac{dn_h}{dt} = \gamma_{eh}n_{Xlh} - \kappa_{ex}n_en_h \\ \frac{dn_{Xhh}}{dt} = \gamma_{Xhh}n_{Xlh} + \kappa_{ex}n_en_h - \kappa_c n_{Xhh}(n_e + n_h) \end{cases}. \quad (5)$$

Here, n_{Xhh} , n_{Xlh} and $n_e = n_h \equiv n$ are two-dimensional densities of heavy and light excitons and the free carriers in the reservoir, respectively.

The system of the equations (5) does not take into account a process of re-ejection of Xhh-excitons out of the light cone into the reservoir, as the radiative lifetime of these excitons is extremely low (~ 10 ps). Correspondingly, their

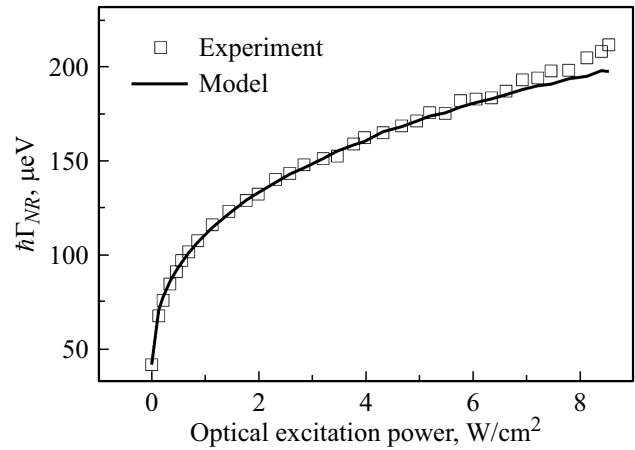


Figure 6. Experimental and theoretically calculated dependences of the nonradiative broadening of the Xhh resonance on the power of continuous excitation in the Xlh.

density is smaller than the density of the excitons in the reservoir by several decimal orders. In principle, this process can arise from absorption of the phonons or scattering the excitons by the free carriers. The estimations show that both mechanisms make a small additional contribution to nonradiative broadening (several percent) at the maximum pumping power used in the experiment.

In case of continuous excitation the system of the equations (5) can be analytically solved (the time derivatives are set equal to zero). The first equation yields

$$x_{Xlh} = \frac{P_{Xlh}}{\gamma_{Xhh} + \gamma_{eh}}. \quad (6)$$

From the second equation we determine the two-dimensional density of the free carriers:

$$n = \sqrt{\frac{\gamma_{eh}}{\kappa_{ex}}} n_{Xlh}. \quad (7)$$

Then, from the third equation, for the two-dimensional density of the heavy excitons in the reservoir we have

$$n_{Xhh} = \frac{\gamma_{Xhh} + \gamma_{eh}}{2\kappa_c n} n_{Xlh} = \frac{1}{2\kappa_c} \sqrt{\frac{\gamma_{Xhh} + \gamma_{eh}}{\kappa_{ex} \gamma_{eh}}} \sqrt{P_{Xlh}}. \quad (8)$$

As one can see from the expression (8), the two-dimensional density of the heavy excitons in the reservoir is proportional to the square root of the pumping rate P_{Xlh} . In turn, the latter non-linearly depends on the power of the optical excitation P_{exc} via the absorption coefficient α_{Xlh} according to the Eq. (4).

The nonradiative broadening of the resonance Xhh is due to the interaction of the photo-generated excitons with all the quasi-particles in the reservoir. However, the estimations show that in the current experimental conditions the two-dimensional density of the heavy excitons in the reservoir significantly exceeds (by dozens and hundreds of times) the densities of other particles (light excitons, free carriers).

That is why the nonradiative broadening is predominantly determined by the two-dimensional density of the heavy excitons

$$\hbar\Gamma_{NR} \approx n_{Xhh}\sigma, \quad (9)$$

where σ is the cross-section of the exciton-exciton scattering. Using the Eqs. (4), (8), (9) and assuming that the σ and rate constants do not depend on the excitation power, we obtain the power dependence of the nonradiative broadening value (see Fig. 6). It is clear that the theoretical calculation agrees well with the experiment.

4. Conclusion

In the high-quality QW heterostructures the resonance lines of the heavy and light excitons, which are observed in the reflectance spectra, can be sufficiently accurately described by applying the non-local dielectric response theory. In particular, smallness of inhomogeneous broadening in the system allows us to determine the main parameters of the resonances with accuracy of fractions of μeV . Such a model system is ideally suited for studying the exciton-exciton interaction.

The theory of dynamic processes has been used to interpret the sub-linear behavior of the nonradiative broadening of the heavy exciton resonance when the power of the optical excitation is increasing. The calculation performed shows full agreement of the theoretical model with the experiment. The result obtained indicates that all the dominant processes are taken into account and the model parameters do not depend on the excitation power at these experimental conditions.

Acknowledgments

The authors would like to thank SPbSU, grant No. 91182694 A.V.M. and I.V.I. thank the Russian Science Foundation for financial support, grant No. 19-72-20039. The authors would like to thank the SPbSU Resource Center „Nanophotonics“ for the experimental sample.

Conflict of interest

The authors declare that they have no conflict of interest.

References

- [1] P.Yu. Shapochkin, S.A. Eliseev, V.A. Lovtcus, Yu.P. Efimov, P.S. Grigoryev, E.S. Khramtsov, I.V. Ignatiev. *Phys. Rev. Appl.*, **12**, 034034 (2019).
- [2] A.V. Trifonov, S.N. Korotan, A.S. Kurdyubov, I.Ya. Gerlovin, I.V. Ignatiev, Yu.P. Efimov, S.A. Eliseev, V.V. Petrov, Yu.K. Dolgikh, V.V. Ovsyankin, A.V. Kavokin. *Phys. Rev. B*, **91**, 115307 (2015).
- [3] M. Combescot, O. Betbeder-Matibet, R. Combescot. *Phys. Rev. Lett.*, **99**, 176403 (2007).
- [4] M. Combescot, M.G. Moore, C. Piermarocchi. *Phys. Rev. Lett.*, **106**, 206404 (2011).
- [5] J.O. Tollerud, S.T. Cundiff, J.A. Davis. *Phys. Rev. Lett.*, **117**, 097401 (2016).
- [6] L.C. Andreani, F. Tassone, F. Bassani. *Sol. St. Commun.*, **77** (9), 641 (1991).
- [7] M.O. Scully, M.S. Zubairy. *Quantum Optics* (Cambridge, Cambridge University Press, 1997).
- [8] E.L. Ivchenko. *Optical Spectroscopy of Semiconductor Nanostructures* (Berlin, Springer, 2004).
- [9] A.V. Trifonov, E.S. Khramtsov, K.V. Kavokin, I.V. Ignatiev, A.V. Kavokin, Y.P. Efimov, S.A. Eliseev, P.Yu. Shapochkin, M. Bayer. *Phys. Rev. Lett.*, **122**, 147401 (2019).
- [10] E.S. Khramtsov, P.A. Belov, P.S. Grigoryev, I.V. Ignatiev, S.Yu. Verbin, Yu.P. Efimov, S.A. Eliseev, V.A. Lovtcus, V.V. Petrov, S.L. Yakovlev. *J. Appl. Phys.*, **119**, 184301 (2016).
- [11] P.S. Grigoryev, A.S. Kurdyubov, M.S. Kuznetsova, I.V. Ignatiev, Yu.P. Efimov, S.A. Eliseev, V.V. Petrov, V.A. Lovtcus, P.Yu. Shapochkin. *Superlatt. Microstr.*, **97**, 452 (2016).
- [12] E.S. Khramtsov, P.S. Grigoryev, D.K. Loginov, I.V. Ignatiev, Yu.P. Efimov, S.A. Eliseev, P.Yu. Shapochkin, E.L. Ivchenko, M. Bayer. *Phys. Rev. B*, **99**, 035431 (2019).
- [13] P.A. Belov. *J. Phys.: Conf. Ser.*, **1482**, 012018 (2020).
- [14] A.S. Kurdyubov, A.V. Trifonov, I.Ya. Gerlovin, B.F. Gribakin, P.S. Grigoryev, A.V. Mikhailov, I.V. Ignatiev, Yu.P. Efimov, S.A. Eliseev, V.A. Lovtcus, M. Assmann, M. Bayer, A.V. Kavokin. *Phys. Rev. B* **104** (3), 035414 (2021).